

Modeling and Simulation of Reacting Systems: A COMSOL Multiphysics Approach for Chemistry Education

Ed Fontes*

Abstract: This article presents a comprehensive overview of modeling and simulation strategies for chemically reacting systems using the COMSOL Multiphysics® software, with a focus on applications in chemical engineering and chemistry education. Beginning with the historical development of the Chemical Reaction Engineering Module and its integration with the CFD Module, we describe how these tools implement the equations of change, reaction kinetics, and thermodynamics for both idealized and spatially resolved systems. The modeling strategy emphasizes a progression from space-independent models to fully coupled multiphysics simulations, illustrated with examples including selective catalytic reduction, heterogeneous catalysis with dual-porosity media, and reacting flow systems in pharmaceutical processes. The use of extra dimensions for intraparticle transport, as well as integration of fluid flow, heat transfer, and chemical reactions, demonstrates the software's capability to address multiscale and multiphysics problems. Finally, we discuss emerging approaches using surrogate models and deep neural networks to accelerate simulations and enable real-time interactivity in the classroom. These methods broaden the pedagogical scope, enabling students – from undergraduate students to graduate researchers – to explore complex reacting systems with greater accessibility, speed, and engagement.

Keywords: Education · Modeling · Simulation · Transport phenomena



Ed Fontes is vice president of development at COMSOL. He was previously the lead developer of the company's transport phenomena modules, including the Chemical Reaction Engineering, Computational Fluid Dynamics (CFD), and Heat Transfer modules. Fontes joined COMSOL in 1999 after five years in research and development in the chemical industry. He holds a PhD in chemical engineering from the Royal Institute of Technology in Stockholm, Sweden, where he specialized in mathematical modeling.

1. How It All Started

The first version of COMSOL Multiphysics (then called FEMLAB) was released in 1998 and quickly attracted attention from the chemical engineering community. For the first time, users could type in equations – using notation similar to pen and paper – and automatically generate numerical models based on the method of lines and finite elements. Problems that once required weeks of coding could now be solved in hours.

In 1999, the Chemical Engineering Module was introduced, providing tutorials and examples that closely followed widely used textbooks such as those by: Fogler; Bird, Stewart, and Lightfoot; Froment and Bischoff; and Wesselingh and Krishna.^[1–4] This alignment with familiar theory, combined with feedback from leading researchers, led to the module being adopted in teaching – even at the undergraduate level. Fogler included COMSOL models in the fourth edition of *Elements of Chemical Reaction Engineering* (2005),^[5] and since then other professors and pioneering users have published books incorporating COMSOL-based models.^[6–10]

The main advantage – then as now – is that students can focus on defining problems, validating models, and interpreting results,

rather than on coding or numerical methods. This deepens their understanding of reacting systems and makes the learning process more engaging.

Subsequent developments included the CFD Module, the Chemical Reaction Engineering Module (2010), which allowed direct input of chemical reactions, and the Application Builder (2014), which enabled educators to create simulation apps for teaching. Together, these tools support a seamless transition from chemical equations to space- and time-dependent reactor models, making advanced modeling accessible at all levels of chemical engineering education (Fig. 1).

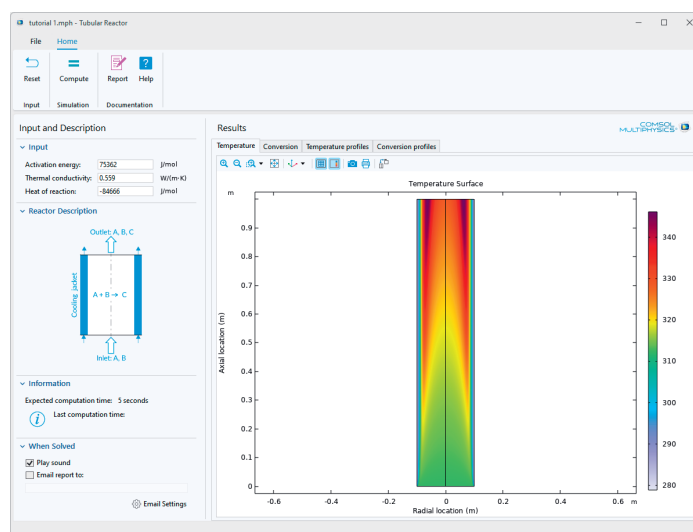


Fig. 1. The Tubular Reactor simulation app created for Fogler's *Elements of Chemical Reaction Engineering*, released in 2014. Students can use the app to vary the activation energy, heat of reaction, and thermal conductivity in a nonideal tubular reactor and then study the resulting conversion and temperature profiles.

*Correspondence: Dr. E. Fontes, E-mail: ed@comsol.com
COMSOL, Stockholm, Sweden

2. Basics of Modeling Chemical Systems

The foundation of mathematical modeling in chemical engineering lies in the equations of change and the principles of reaction kinetics and thermodynamics. The equations of change describe mass, momentum, and energy balances for space- and time-dependent models.^[2] Fig. 2 shows how these concepts are implemented in the Chemical Reaction Engineering Module and the CFD Module used with COMSOL Multiphysics.

To explain the implementation in these modules, a few fundamental relationships are necessary.

2.1 Conservation Equations

Consider a conserved quantity ϕ with a flux vector $\mathbf{j} = (j_x, j_y, j_z)$. The quantity ϕ may represent mass, energy, or momentum. A balance for ϕ can be derived by examining a small volume element of dimensions Δx , Δy , and Δz over a small time interval Δt , where \mathbf{j} is in units of quantity per unit area per unit time and the production or consumption term R_s is in units of quantity per unit volume per unit time. Taking the limits $\Delta x, \Delta y, \Delta z, \Delta t \rightarrow 0$ yields the equation of change:

$$\frac{\partial \phi}{\partial t} + \nabla \cdot \mathbf{j} = R_s \quad (1)$$

This conservation equation must hold in every infinitesimal volume element of the continuum (fluid or solid) in the system. It is called ‘partial’ because it describes changes with respect to one independent variable at a time (x, y, z , or t). This general form can express the conservation of momentum, energy, and mass in transport phenomena modeling.

For momentum conservation, ϕ is a vector, and its flux is a tensor that includes the stress tensor. Combining the momentum balance with the constitutive equations for momentum flux and the conservation of mass for an incompressible Newtonian fluid gives the Navier–Stokes equations, which forms the basis of CFD modeling. For energy conservation, substituting energy for ϕ in Eqn. (1) yields the heat transfer equation.

For mass transport, we apply Eqn. (1) to each chemical species i in a reacting fluid, where the conserved quantity is the concentration c_i and the flux is \mathbf{N}_i . For a dilute solution, the conservation equation becomes:

$$\frac{\partial c_i}{\partial t} + \nabla \cdot \mathbf{N}_i = R_i \quad (2)$$

If mass transport occurs only by diffusion and Fick’s law applies, $\mathbf{N}_i = -D_i \nabla c_i$, we obtain the diffusion–reaction equation:

$$\frac{\partial c_i}{\partial t} + \nabla \cdot (-D_i \nabla c_i) = R_i \quad (3)$$

When convection (bulk flow) is present, the convection–diffusion–reaction equation applies:

$$\frac{\partial c_i}{\partial t} + \nabla \cdot (-D_i \nabla c_i + c_i \mathbf{u}) = R_i \quad (4)$$

where \mathbf{u} is the velocity vector.

2.2 Reaction Kinetics and Thermodynamics in COMSOL Multiphysics

The Chemical Reaction Engineering Module also provides tools for simulating perfectly mixed (space-independent) systems or for highly controlled systems - for example, ideal plug flow reactors (PFR). In this interface, users can enter chemical reactions in standard chemical notation. The software can then:

- Automatically generate material and energy balances for the system (including space-dependent models if needed).
- Derive kinetic expressions for elementary reactions from the law of mass action.
- Allow user-defined expressions for reaction rates as functions of species concentrations, temperature, and other variables.

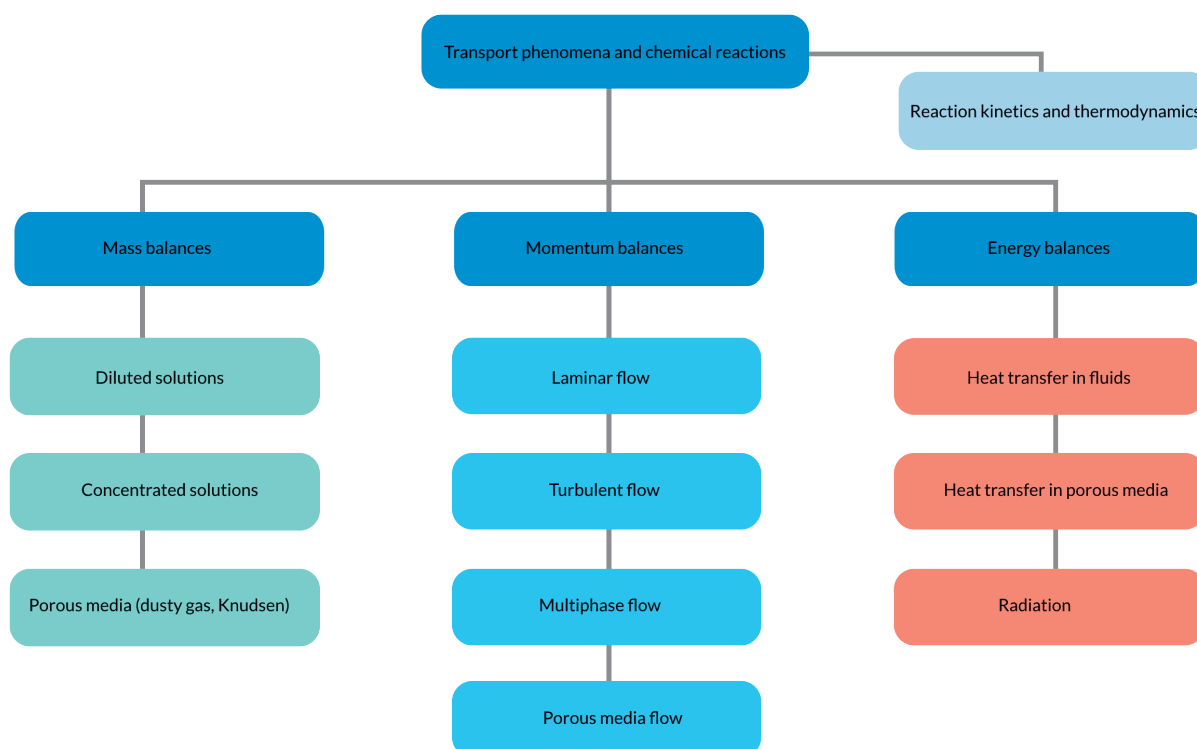


Fig. 2. The main structure of the Chemical Reaction Engineering Module and the CFD Module. Combinations, such as multiphase flow formulations, are available for laminar and turbulent flow. There are also several models for multicomponent transport, both in free and porous media.

These balances and kinetic expressions produce ordinary differential equations (ODEs) for ideal reactors. For an ideal batch or continuous stirred tank reactor (CSTR), solving the ODEs yields the time evolution of the mixture's composition. For ideal PFRs, a steady state, solving the equations yields the composition along the axial direction of the reactor (each cross-sectional slice perpendicular to the axial direction is perfectly mixed) (Fig. 3).

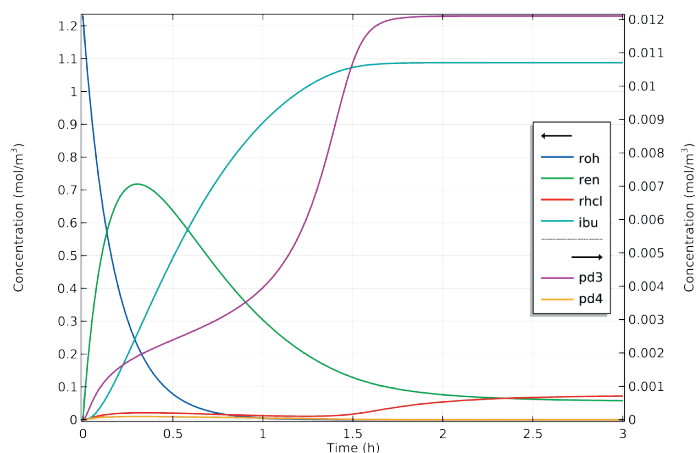


Fig. 3. Simulation results for a perfectly mixed batch reactor, shown here for an ibuprofen synthesis. The plot shows that the synthesis is completed after about 2 h.

2.3 Space-Independent Models

For space-independent systems, the spatial-derivative terms in the equations of change vanish. For example, applying this to Eqn. (4) for a chemical species in an ideal batch reactor yields:

$$\frac{dc_i}{dt} = R_i \quad (5)$$

A similar equation defines the energy balance for such system:

$$\rho C_p \frac{dT}{dt} = Q \quad (6)$$

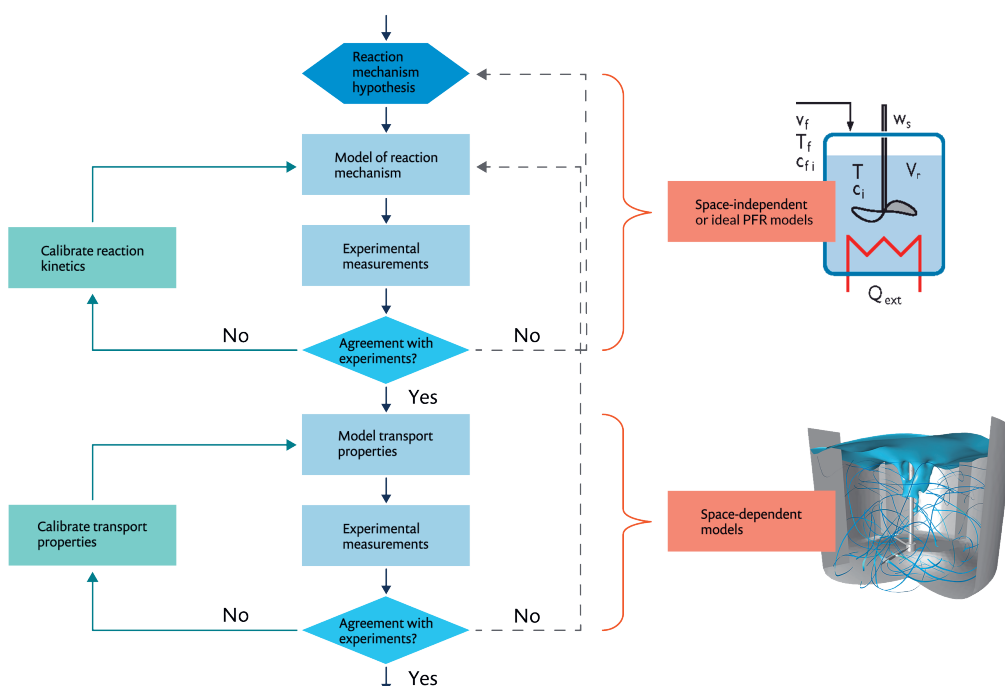


Fig. 4. Suggested modeling strategy.

2.4 Numerical Models

In COMSOL Multiphysics, the equations of change are expressed symbolically and then discretized on the fly using finite element methods combined with the method of lines. This symbolic approach makes it straightforward to define custom kinetic expressions, since the equation interpreter can parse any function of the model's dependent variables (*e.g.* concentrations, temperature, and activities). ODEs from space-independent models are solved using a number of established numerical methods.

3. The Modeling Strategy

Transport and reaction processes often involve multiple dependent variables (*e.g.* concentrations, flow velocity, pressure, and temperature) that are nonlinearly coupled in both the transport equations and the reaction terms (often expressed as source or sink terms in the equations of change). This complexity is also reflected in experiments, where it can be difficult to isolate the effects of individual operating conditions unless the experiments are highly controlled.

A common approach is to first study the system under perfectly mixed conditions, achieved either by vigorous stirring or by using microfluidic systems (*e.g.* single-channel PFRs), where uniform conditions are easier to maintain. This approach is also recommended when using the Chemical Reaction Engineering Module, either alone or in combination with the CFD Module.

Fig. 4 shows a typical and effective modeling strategy. The first step is to create a model of the reacting system under perfectly mixed or otherwise well-controlled conditions. In real experiments, this means that measurements of composition and temperature at one location are representative of the entire volume (batch reactors and CSTRs) or of a perfectly mixed cross section (PFRs). In the model, the governing equations are ODEs, which are simpler and less computationally demanding than the PDEs that include spatial transport phenomena. Such models are easier to solve, validate against experimental data, and optimize for objectives such as maximum conversion or minimal byproduct formation.

The Reaction Engineering interface supports this approach. Users can enter chemical reactions either in symbolic form (*e.g.* $A + B \rightarrow C + D$) or as full chemical formulas

(e.g. $\text{CH}_4 + \text{H}_2\text{O} \rightarrow \text{H}_2 + \text{CO}_2$). When chemical formulas are used, the interface automatically identifies the elements and verifies that the atom balances and stoichiometry are correct. By default, the tool applies the law of mass action to generate reaction-rate expressions. If the user chooses to include the energy balance, the model will also predict the temperature of the reacting system as a function of time.

As an example, consider a PFR for NO_x and ammonia conversion in a monolithic reactor (Fig 5), such as those used in diesel engines for exhaust gas treatment. The purpose of the reactor is to perform selective catalytic reduction (SCR) of harmful nitrogen oxides (NO and NO_2) into nitrogen (N_2) in the exhaust system of a heavy-duty diesel truck.

▼ Reaction Formula
Balance

Formula:

Reaction type:

Irreversible
▼

$$R_i = \sum_j \nu_{ij} r_j$$

▼ Reaction Rate

Mass action law
▼

$$r_j = k_j^f \prod_{i \in \text{react}} c_i^{-\nu_{ij}}$$

Overall forward reaction order: 2

▼ Rate Constants

Use Arrhenius expressions

$$k^f = A^f \left(T/T_{\text{ref}} \right)^{n^f} \exp\left(\frac{-E^f}{R_g T} \right), T_{\text{ref}} = 1\text{K}$$

Forward frequency factor:

Forward temperature exponent:

Forward activation energy:

Fig. 5. Settings window for a reaction used in a simple tutorial.

Ammonia is injected upstream of the after-treatment system, which consists of a catalytic monolithic reactor with two beds containing different catalysts. The upstream bed is the SCR bed, which selectively converts NO_x to nitrogen. The second bed is the ammonia-slip catalyst (ASC), which converts any remaining ammonia to nitrogen.

In the SCR bed (Fig. 6), six reactions occur: three desired heterogeneous reactions (Eqns. (7)–(9), which occur on the cat-

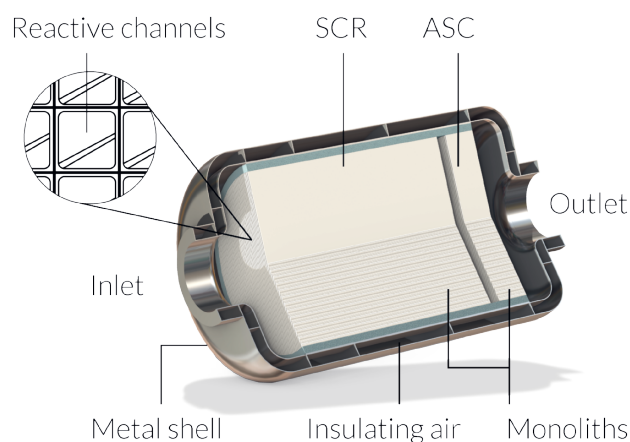
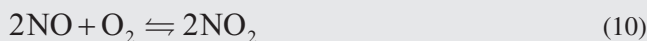
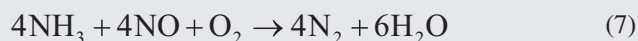
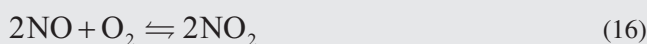


Fig. 6. Schematic drawing of the 3D reactor. The reactor is about 74 cm from inlet to outlet. Since the geometry is axisymmetric, a 2D axisymmetric model can be used.

alyst surface); one homogeneous oxidation of nitrogen monoxide (Eqn. 10); and two undesired reactions (Eqns. 11–12).



In the ASC bed, there is one desired reaction (Eqn. (13)), two undesired reactions (Eqns. (14)–(15)), and one homogeneous equilibrium reaction (Eqn. (16)).



The reactions in Eqns. (7)–(16) are overall (sum) reactions and do not represent the full kinetic mechanism; thus, mass action expressions based solely on these reactions would not be appropriate. Instead, empirical rate expressions are used for each reaction.

For example, the rate expression for reaction (7) is:

$$r_7 = k_{f1} \left(\frac{c_{NO} c_{O_2} c_{NH_3}}{1 + K_{NH_3} c_{NH_3}} \right) \quad (17)$$

This rate expression can be entered directly into the user interface, as shown in Fig. 7. In the Reaction Rate field, the concentration of NO is written as `re.C_NO`. Since all the reactions are temperature dependent, and because we are interested in the temperature profile along the PFR, the rate constants are defined using the Arrhenius equation.

Fig. 7. Settings window of the Reaction Engineering interface. Reactions are entered directly in the Formula field, where => defines an irreversible reaction and <=> defines a reversible reaction. Kinetics expressions correspond to the equations discussed previously, with species concentrations referenced directly (e.g. `re.C_NO` for nitrogen monoxide). The software automatically generates the mass and energy balances by parsing the chemical equation, so no manual variable declarations are needed.

3.1 Results from the Ideal Model

The plot in Fig. 8 shows the conversion in the PFR at both low engine loads (small inlet flow) and high engine loads (large inlet flow). The Fig. reveals that the highest emissions of NO_x and ammonia occur at the lowest engine load. This is due to the lower temperature, which reduces the reaction rate. Even though the incoming gas contains less NO_x and the total flow rate is lower, the reaction rate is simply insufficient under these conditions.

Once the ideal PFR model has been validated – here by comparison with published experimental data – it can be extended to include radial effects. This is done by selecting the Generate Space-Dependent Model button and specifying the geometry dimensions and relevant transport phenomena; in this case, transport of dilute chemical species, fluid flow in porous media, and heat transfer in porous media. The software automatically transfers the governing equations and properties from the 1D model to the new 2D axisymmetric model. The only additional steps are creating the geometry and defining the boundary conditions.

This transition from the idealized 1D model to a spatially resolved 2D model enables the study of temperature and concentra-

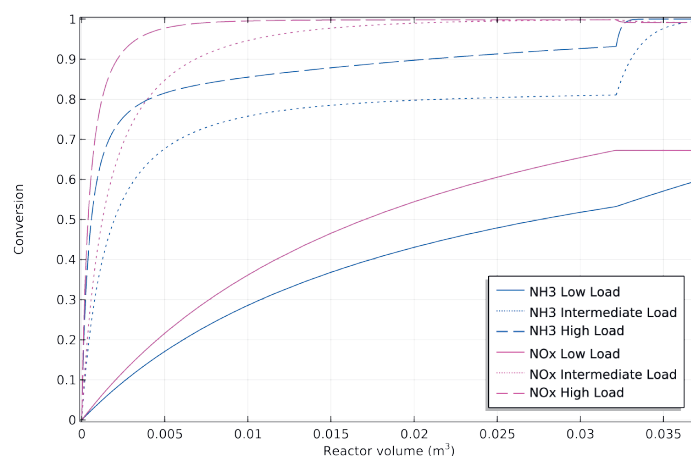


Fig. 8. Conversion of NH_3 and NO_x along the length of the reactor for the ideal PFR at low and high engine loads.

tion gradients across the reactor cross section – effects that can be significant under real operating conditions and are addressed in the next section.

3.2 Results from the Model That Account for Radial Variations

The corresponding plot for the 2D axisymmetric model is shown in Fig. 9. This plot reveals that radial variations in the reactor are more pronounced at low engine loads. At higher inlet flows, the temperature rises, and the entire monolith reaches a more uniform temperature. Under high load conditions, the simple 1D PFR model agrees well with the results from the 2D axisymmetric model. However, at lower temperatures, both temperature and concentration gradients in the radial direction become more significant, leading to poorer agreement between the two models.

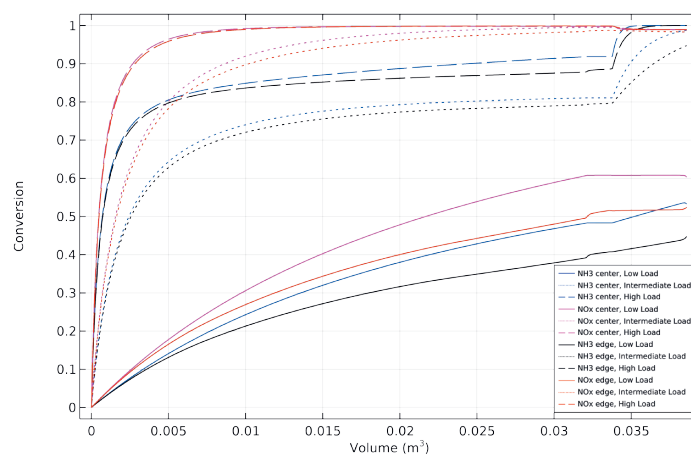


Fig. 9. Conversion of NH_3 and NO_x along the length of the reactor, shown at the reactor center and near the outer radius, for low and high engine loads.

The advantage of the 2D axisymmetric reactor model is that it not only resolves radial variations in concentration and temperature, but it can also be used to assess the impact of the reactor's metal shell and insulation. The results from the 2D simulation can be used to validate the 1D model and compute effective, lumped heat transfer properties for use in the simpler model. A refined and validated 1D model can then be incorporated into a system-level model of the entire engine, where a 2D axisymmetric approach would be computationally prohibitive. This practice of using more

detailed models to validate and parameterize simpler models is an important concept for students, as it is widely applied in chemistry and chemical engineering.

Despite the complexity of both the 1D PFR and 2D axisymmetric reactor models, the entire setup can be created directly in the COMSOL Multiphysics user interface – no programming or external scripting required. Building the model from scratch takes about an hour and solving the 2D axisymmetric equations (including a parametric sweep of the inlet velocity) takes less than a minute on a desktop computer. This makes the model highly suitable for use in chemical-engineering computer lab sessions. We use this example in our introduction to the Chemical Reaction Engineering Module because it covers all essential steps for mastering the software: from generating thermodynamic and kinetic data to modeling both ideal and nonideal reactors (Fig. 10).

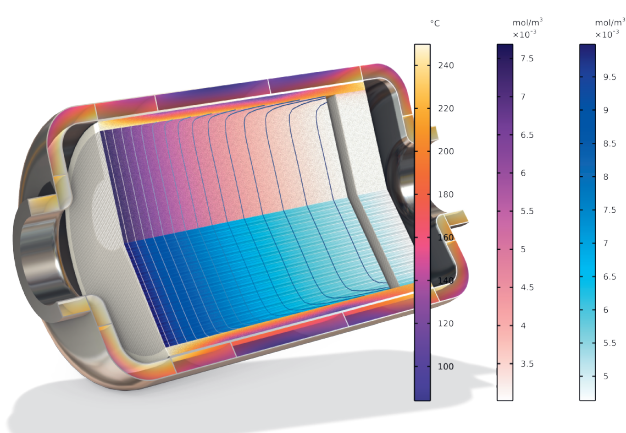


Fig. 10. Temperature and composition in the space-dependent model at a low load. The violet-shaded scale and contours represent the sum of NO and NO₂, while the blue-shaded scale represents the NH₃ concentration.

4. Heterogeneous Catalysis and the Concept of Extra Dimensions

Heterogeneous catalysis is relatively straightforward to describe at the microscale: Reactant molecules are transported to a catalyst surface, adsorb, undergo a surface reaction facilitated by changes in their free energy upon adsorption, desorb, and are transported away. At the scale of a catalyst bed, such as in the example previously discussed, modeling becomes more complex. Because we typically cannot resolve every pore and surface detail, the porous domain is homogenized, introducing effective properties such as porosity, tortuosity, and specific surface area (surface area per unit volume of catalyst).

The complexity increases when the catalyst is composed of packed porous particles. In this case, there are two distinct pore scales: the interparticle pores (between the particles) and the intraparticle pores (within each particle). This naturally leads to a two-scale description: one at the particle scale and one at the bed scale (Figs. 11 and 12).

The first formal models and theory for such dual-porosity catalysts were introduced by Thiele^[11] and later generalized by Aris.^[12] In this framework, the intraparticle diffusion–reaction problem (particle scale) can be solved analytically in certain cases, with the resulting expressions for Thiele’s modulus and the effectiveness factor used as effective reaction terms in the bed-scale reaction–diffusion equations. Analytical solutions are only straightforward for a single reacting species and simple reaction mechanisms. As a graduate student in chemical engineering, I re-

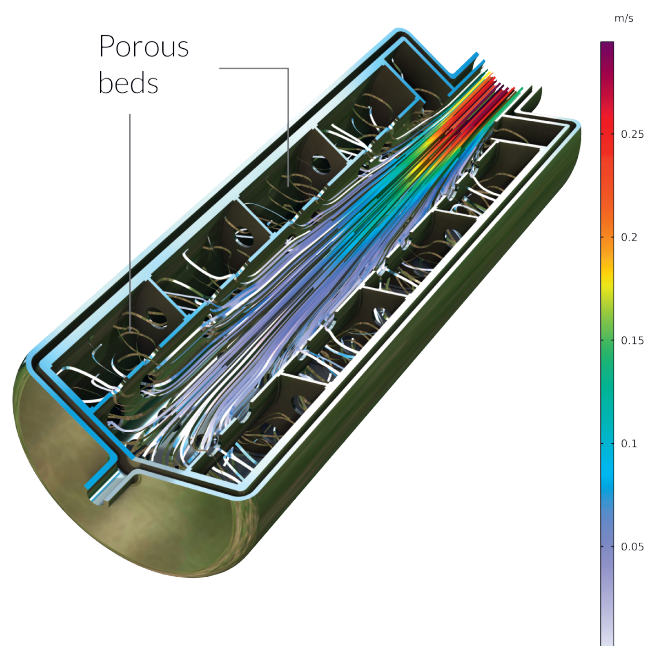


Fig. 11. Flow velocity in a metal hydride tank for hydrogen storage. In the porous metal beds, adsorption occurs during recharge and desorption occurs during discharge.

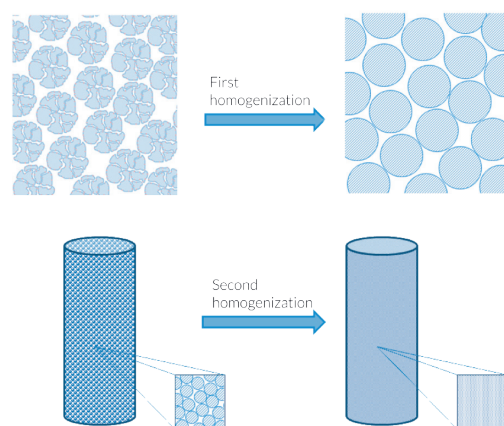


Fig. 12. In the theory developed by Thiele and Aris, homogenization is performed in two stages: first at the particle scale and then at the bed scale.

call spending a considerable amount of time solving such problems by hand.

In the Chemical Reaction Engineering Module, we address the intraparticle transport–reaction problem by introducing an extra dimension representing the radial coordinate inside the catalyst particles. This dimension is discretized using finite elements, enabling the use of any kinetic expression for the heterogeneous reactions inside the particles, fully coupled with the equations of change at the bed scale (Fig. 13). Time-dependent problems can also be solved inside the particles, allowing the study of a much wider range of cases, such as shrinking core problems^[13] including complex reaction kinetics. Traditionally, the theoretical and modeling aspects of heterogeneous catalysis are introduced only at the graduate level in chemistry and chemical engineering. Using the Chemical Reaction Engineering Module, these concepts can be taught much earlier, since students do not need to know the technicalities of solving multi-scale problems manually.

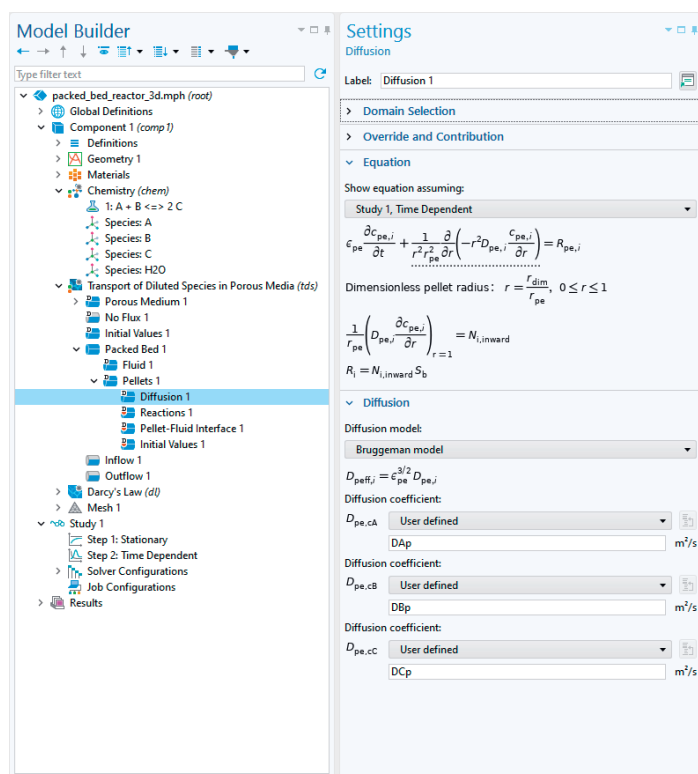


Fig. 13. The model builder tree for a tutorial model of a packed bed in 3D and the settings window for diffusion inside catalyst pellets. The model treats a system of three reacting chemical species and one solvent (H₂O). Different diffusion models can be selected, such as Bruggeman, Millington–Quirk, or tortuosity-based models.

5. CFD and Reacting Flow

The field of computational fluid dynamics (CFD) has deep roots in chemical engineering, with several of the most widely used CFD software packages originating in chemical engineering departments.^[14] Despite this history, CFD tools are still not fully integrated into undergraduate-level courses in either chemistry or chemical engineering. However, increasing computing power and the improved usability of modeling tools are changing this issue. Today, the Chemical Reaction Engineering Module and the CFD Module are frequently used in undergraduate transport phenomena courses. In chemistry curricula, transport phenomena and CFD are most often introduced in the contexts of electrochemistry and heterogeneous catalysis (as in the examples mentioned previously). The growing importance of transport modeling in environmental chemistry, cleantech, and pharmaceutical processes is accelerating this trend.

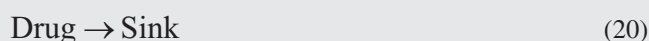
A major advantage of combining the Chemical Reaction Engineering Module with the CFD Module is the ability to move seamlessly from chemical equations, with validated reaction kinetics and thermodynamics, to complete models that also include fluid flow and heat transfer.

The following example from the pharmaceutical industry illustrates this approach for the production of antibody–drug conjugates (ADCs). ADCs are produced in a conjugation process where an antibody with attached linkers reacts with a drug molecule. In this case, the antibodies are monoclonal antibodies (mAb): engineered proteins that closely resemble human antibodies and are therefore processed by the body in a similar way. Mimicking natural antibodies, mAbs bind only to their specific target antigen, making them ideal for targeted therapeutic delivery - for example, in oncology.

After producing the monoclonal antibody with the linker, the drug is attached to the antibody *via* the linker molecule in a

stirred-tank reactor, operated in either batch or semibatch mode. In this example, a semibatch process is modeled under isothermal conditions. The mAb has two binding sites, and the reaction is site directed. At the start of the process, the tank contains a dilute solution of mAb. The drug is added through a dip tube with an outlet located near the stirrer. The feed rate and duration are specified, and after feeding stops, the reactions proceed until the desired conversion is achieved. The objective is to obtain a homogeneous, stable conjugate without aggregation.

The first conjugation step is:



The simulation produces both the turbulent fluid flow field and the spatial concentration profiles in the reactor. Product quality depends strongly on the conjugation process, with key factors including antibody concentration, linker-to-drug ratio, and process time. The model can also be used to study the influence of stirrer speed, feed rate, and reactor geometry. The space-dependent results can be compared with those from a perfectly mixed model, which – after validation – can be used for parameter estimation and optimization.

The fully resolved 3D CFD model involves rotating domains and millions of time-dependent equations solved at each time step. Such simulations may require hours or even days to complete. However, defining the model using chemical equations and performing a lower-resolution run to verify correctness typically takes only a few hours. These types of problems are well suited for inclusion in bachelor-level projects in chemistry or chemical engineering, even for second-year students.

6. Surrogate Models, DNNs, and the Future

Today's students are accustomed to chatbots, mobile apps, and photorealistic computer games that simulate reality with impressive accuracy. In that context, the idea that a reactor simulation might take hours causes disappointment and frustration. When using a simulation app, such as the one shown in Fig. 1, the solution can take only a few seconds. This can set expectations that all simulations should deliver instant results.

Surrogate models offer a way to meet these expectations while preserving the accuracy of high-fidelity simulations. Even a model like the one in Fig. 14, with millions of degrees of freedom, can be approximated using a surrogate model trained on data from the original model. Deep neural networks (DNNs) are one effective approach: Training requires an initial investment of time and computing power, but once trained, the surrogate can produce near-instant predictions for complex 3D transport and reaction problems, provided the inputs stay within (or close to) the parameter space used for training.

This capability leads to significant opportunities for teaching. In undergraduate courses, advanced modeling could be used live in the classroom. In graduate courses and for thesis projects, surrogate models could enable rapid parameter sweeps, sensitivity analysis, uncertainty quantification, and extensive optimization studies. To illustrate, we adapted our original tubular reactor app (Fig. 1) to include a surrogate model. The updated version (Fig. 15) adds interactive sliders for input param-

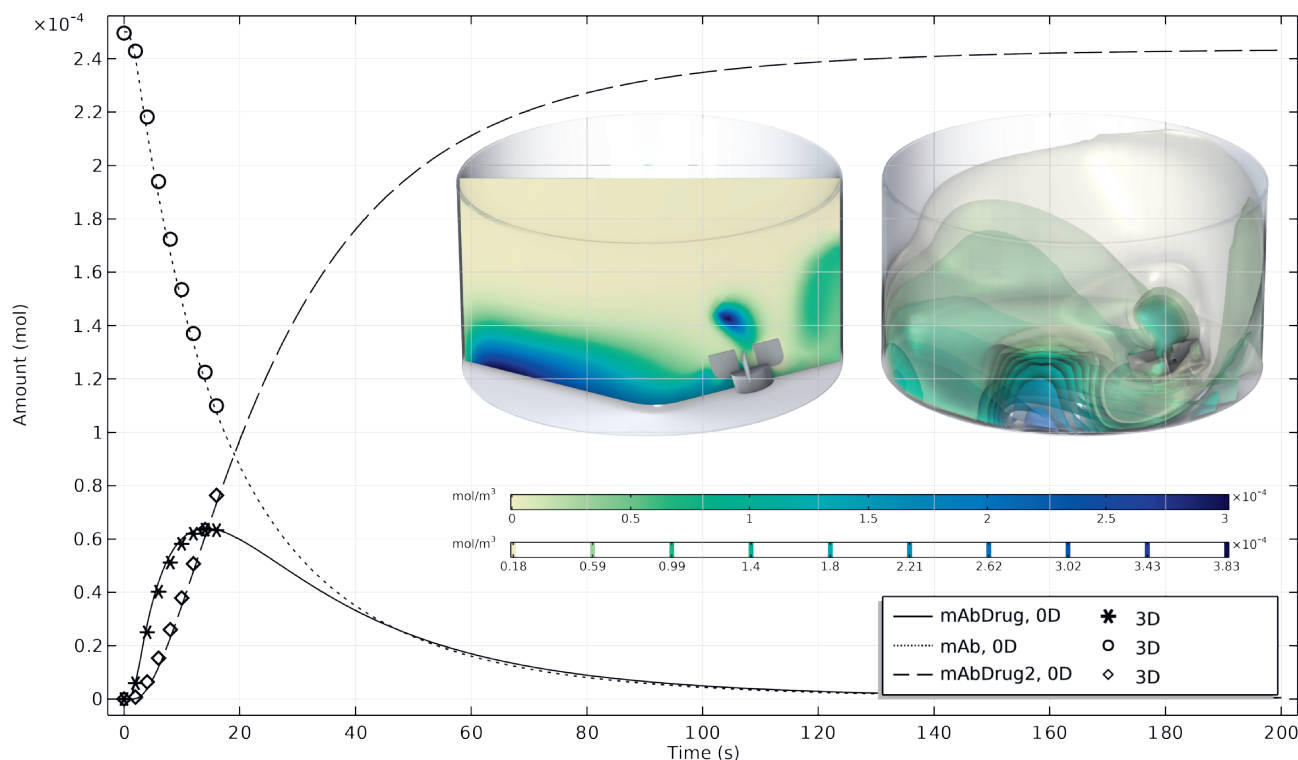


Fig. 14. Total amount of each species in the tank reactor, comparing results from the full 3D reacting flow model with those from an ideal semibatch tank reactor model.

eters, with the solution updating in real time as students adjust them.

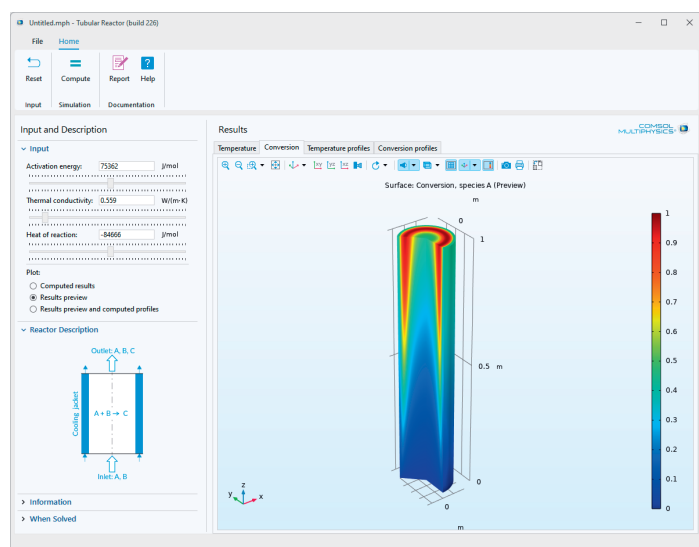


Fig. 15. The tubular reactor app from Fig. 1, augmented with a surrogate model that produces instant results within the trained parameter space.

By using simulation data to train DNNs, accurate surrogate models can be created for use even by first-year students. This approach will not replace in-depth theoretical analysis or the need to understand mathematical modeling, but it can provide a shorter path to intuitive understanding for students. The immediacy of the results can also make learning more engaging and enjoyable – perhaps in the same way that computer games captivate their players. In a way, we are now using trained DNNs to help train students' own neural networks.

Received: August 25, 2025

- [1] H. S. Fogler, 'Elements of Chemical Reaction Engineering', 4th ed., Prentice Hall, **2005**.
- [2] R. B. Bird, W. E. Stewart, E. N. Lightfoot, 'Transport Phenomena', 1st ed., John Wiley & Sons, **1960**, <https://doi.org/10.1002/aic.690070245>.
- [3] G. F. Froment, K. B. Bischoff, 'Chemical Reactor Analysis and Design', 2nd ed., John Wiley & Sons, **1990**.
- [4] R. A. Wesselingh, R. Krishna, 'Mass Transfer', Ellis Horwood, **1990**.
- [5] COMSOL AB, 'Elements of Chemical Reaction Engineering: COMSOL Models', [Online]. <https://www.comsol.com/ecre>.
- [6] B. A. Finlayson, 'Introduction to Chemical Engineering Computing', John Wiley & Sons, **2006**, <https://doi.org/10.1002/0471776688>.
- [7] J. O. Wilkes, 'Fluid Mechanics for Chemical Engineers with Microfluidics and CFD', 2nd ed., Prentice Hall, **2005**, <https://doi.org/10.5860/choice.36-3354>.
- [8] W. B. Zimmerman, 'Multiphysics Modeling with Finite Element Methods', World Scientific, **2006**, <https://doi.org/10.1142/6141>.
- [9] J. L. Plawsky, 'Transport Phenomena Fundamentals', 2nd ed., CRC Press, **2009**, <https://doi.org/10.1201/9781439882122>.
- [10] K. J. Beers, 'Numerical Methods for Chemical Engineering: Applications in MATLAB', Cambridge University Press, **2007**.
- [11] E. W. Thiele, *Ind. Eng. Chem. Res.* **1939**, *31*, 916, <https://doi.org/10.1021/ie50355a027>.
- [12] R. Aris, 'Introduction to the Analysis of Chemical Reactors', Englewood Cliffs, NJ: Prentice-Hall; **1965**, <https://doi.org/10.1002/aic.690120202>.
- [13] C. Moreno-Pulido, R. Olwande, T. Myers T, F. Font, *arXiv* **2025**, <https://doi.org/10.48550/arXiv.2507.21042>.
- [14] NAFEMS, 'The Origins of Fluent', <https://www.nafems.org/blog/posts/analysis-origins-fluent/> (accessed August 15, 2025).

License and Terms



This is an Open Access article under the terms of the Creative Commons Attribution License CC BY 4.0. The material may not be used for commercial purposes.

The license is subject to the CHIMIA terms and conditions: (<https://chimia.ch/chimia/about>).

The definitive version of this article is the electronic one that can be found at <https://doi.org/10.2533/chimia.2025.698>